JACS
JOURNAL OF THE AMERICAN CHEMICAL SOCIETY

Communication

pubs.acs.org/JACS

Enhanced Electrochemical Expansion of Graphite for *in Situ* Electrochemical Functionalization

Yu Lin Zhong and Timothy M. Swager*

Department of Chemistry and Institute for Soldier Nanotechnologies, Massachusetts Institute of Technology, 77 Massachusetts Avenue, Cambridge, Massachusetts 02139, United States

Supporting Information

ABSTRACT: An all electrochemical route to functionalized graphene directly from a graphite electrode is described herein obviating the need for defect inducing oxidative or prolonged sonication treatments. Enhanced electrochemical expansion of graphite is achieved by sequential treatment, beginning with the established method of expansion by electrolysis in a Li^+ containing electrolyte, and then with the much larger tetra-*n*-butylammonium. The result is a hyperexpansion of the graphite basal planes. As a demonstration of the utility of this method, we successfully performed a subsequent *in situ* electrochemical diazonium functionalization of the hyperexpanded graphite basal planes to give functional graphene sheets. This potential controlled process is more effective than chemical processes and also provides a means of controlling the degree of functionalization. We have further demonstrated that the functionalized graphene could be converted to a pristine low defect form via laser ablation of the funtional groups. As a result, this method presents a potentially scalable approach for graphene circuit patterning.

The intense research focus on graphene can be in large part attributed to its exceptional electronic properties first observed on the adhesive tape exfoliated graphene by Novoselov and co-workers.[1] To realize the technological potential of graphene, new versatile processes to create low defect graphene from abundant and inexpensive carbon sources have been pursued based on a variety of potential target applications.[2,3] For high-end electronic applications, graphene produced by chemical vapor deposition (CVD)[4] or by epitaxial growth[5] are presently the most suitable choices despite the higher cost associated with these production methods. For applications seeking to exploit other outstanding properties of graphene (e.g., optical, mechanical, barrier, and surface area), lower cost bulk chemical production of graphene from graphite via the graphene oxide route has received the most attention.[6,7] However, a limitation of the latter route is the generation of defective graphene basal planes (vacancy defects) resulting from the exceptionally harsh oxidizing conditions that cannot be completely repaired effectively even after thermal or chemical reduction.[8]

Alternative nonoxidative routes to the chemical production of graphene include the use of solvent/surfactant-assisted liquid exfoliation of graphite,[9,10] the formation of graphite intercalated compounds (GICs),[11−13] and electrochemical methods.[14,15] There are drawbacks and limitations with each method, but the primary limiting factor has been the relatively low yields of single-layer graphene (SLG), and the inability of the methods to compete with the strong $\pi-\pi$ intersheet interactions that favor stacked graphite sheets and deintercalation processes. Furthermore, the use of reactive intercalators such as sodium and potassium metals precludes the attachment of many functional groups in the subsequent chemical functionalization step. The high yield synthesis of few-layer graphene (FLG) flakes through electrochemical expansion of graphite was recently developed by Loh and co-workers but an additional prolonged power sonication step was required and the associated mechanical breakdown limits the size of graphene flakes.[15] In our present work, we demonstrate enhancement through a two step process wherein graphite is first activated in Li^+ containing electrolytes and then further activated/expanded by additional activation in tetra-*n*-butylammonium (TBA) electrolytes. This enhanced expansion of the graphite allows for functionalization of individual graphene sheets and we demonstrate *in situ* electrochemical functionalization of the expanded graphite foil with the postaddition of aryldiazonium salts.

The activation of graphite begins with the immersion of a thin strip of graphite foil in propylene carbonate containing lithium perchlorate and a voltage ramp to −5 V (vs Pt mesh) (see Supporting Information for experimental details). In this preconditioning step, the graphite foil observably expanded along its *c* axis due to the co-intercalation of propylene carbonate with lithium ions and the well-known concomitant electrodecomposition to form a solid-electrolyte-interphase (SEI) layer with evolution of propylene gas (Scheme 1).[16] The graphite foil ceased to expand beyond the application of −5 V as the graphite lattice became fully charged with lithium ions. Notably, the application of more negative voltages likely resulted in the electrolysis of lithium perchlorate and the electrodeposition of lithium metal on the graphite as evidenced by the formation of a greyish coating.

In the second step, tetra-*n*-butylammonium perchlorate is added into the electrolyte solution and applied potential is maintained at −5 V for 24 h, and a physical increase in the size of the expanded graphite is observed (Scheme 1). Although a two-electrode system does not allow for precise control of the potential applied to the graphite, we find that the potential was

Received: September 11, 2012
Published: October 17, 2012

   dx.doi.org/10.1021/ja309023f | *J. Am. Chem. Soc.* 2012, 134, 17896−17899

Scheme 1. Schematic and Images of Electrochemical Expansion of Graphite

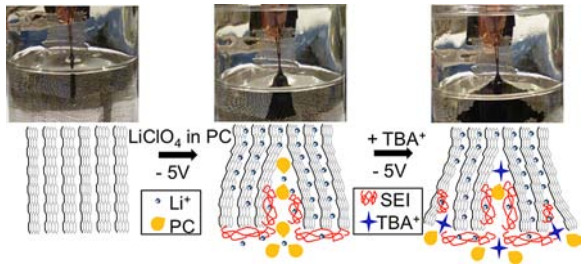

relatively constant at −3.0 ± 0.5 V vs standard calomel electrode. During this enhanced electrochemical expansion step, it appears that positively charged TBA cations penetrate into the graphite lattice by cation exchange with the intercalated lithium ions.[17] However, an additional critical factor is the electrodecomposition of the intercalated TBAs (Figure S1)[18] which partially neutralizes the positive charges within the graphite lattice and thereby continually maintains a driving force for intercalation of TBA cations. This process is inferred from the lack of graphite expansion when the applied voltage is less than the electrodecomposition potential of TBA (−2.5 V vs standard calomel electrode). Similarly, there is also a concomitant electrodecomposition of propylene carbonate molecules (solvating the TBA cations) resulting in a constant generation of SEI layers (Scheme 1), which are known to act as physical spacers within the graphite lattice. The identity of the SEI layer is confirmed by X-ray photoelectron spectroscopy (XPS) to consist of lithium alkyl carbonates. The SEI layer can be removed by extensive washing as evident in the significantly reduced XPS O1s peak (Figure 1a). In addition to the small

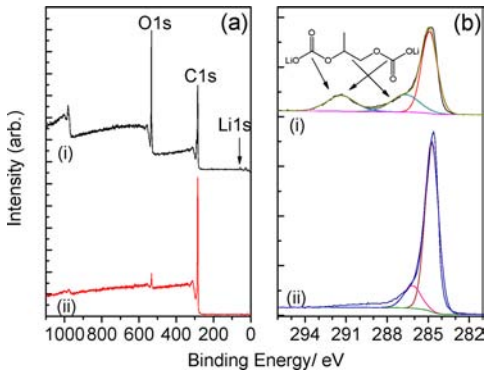

Figure 1. (a) XPS survey scans and (b) C1s XPS spectrum of electrochemically expanded graphene (i) after rinsing once with DMF and (ii) after extensive washing.

XPS O1s peak, the small shoulder in the XPS C1s at around 286.2 eV (Figure 1b(ii)) indicates that there may be a small degree of covalently linked alcohol or ether functional groups or residual solvent molecules trapped between the graphene sheets. After the full electrochemical expansion of graphite foil, the electrochemically expanded graphene (EEG) was subjected to the *in situ* electrochemical functionalization with aryldiazonium salts to obtain the electrochemically functionalized graphene (EFG). We have focused on reactions with 4-bromobenzenediazonium tetrafluoroborate because the bromide provides a chemical marker for XPS analysis and this reagent demonstrates the compatibility of our method toward a reductively sensitive functional group. For comparison, we performed a chemical functionalization on the EEG by first dispersing the EEG in dimethylacetamide (DMAc) followed by addition of the aryldiazonium salt to obtain the chemically functionalized graphene (CFG). As a control experiment, we performed the electrochemical functionalization on the EEG without the addition of TBA salts. After functionalization, the solids are rinsed with acetone, 50% ethanol, dichloromethane and dimethylformamide and the EFG is then dispersed in 200 mL of dimethylformamide (DMF) and the supernatant (about 170 mL) was collected after centrifugation at 1000 rpm for 30 min. It is expected that noncovalent oligomeric materials from aryldiazonium salt decomposition will be removed in these processes. As shown in Figure 2a, it is obvious that the

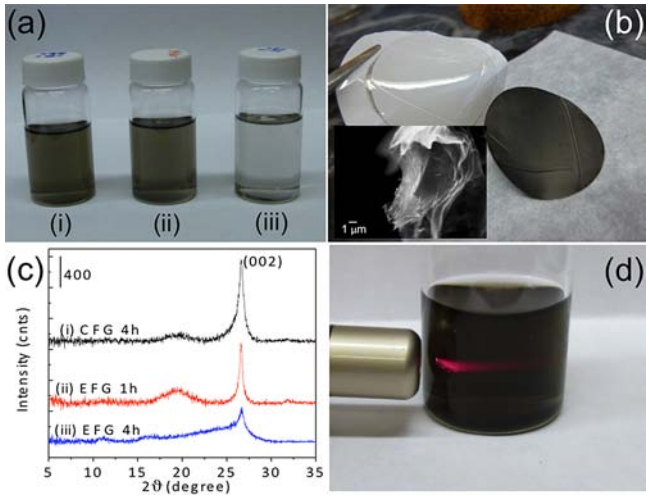

Figure 2. (a) Photograph showing supernatant of (i) chemically functionalized graphene (CFG), (ii) electrochemically functionalized graphene (EFG) and (iii) control in DMF after centrifugation. (b) Photograph showing flexible free-standing EFG film peeled off from polycarbonate filter membrane. The inset shows SEM micrograph of EFG film edge. (c) X-ray diffraction (XRD) pattern of (i) CFG film with reaction time of 4 h and EFG film with reaction time of (ii) 1 h and (iii) 4 h. (d) Photograph of concentrated (0.1 mg/mL) EFG dispersion in DMF after three weeks of standing displaying Tyndall effect.

supernatants of the CFG and EFG were homogeneously dark with concentrations over 20 μg/mL (Table 1) as compared to the clear supernatant from the control procedure. These results suggest that the addition of the TBA salts results in the hyperexpansion of graphite such that individual graphene sheets are functionalized. Flexible free-standing EFG films could be obtained by filtration of the EFG dispersion (Figure 2b). These films contain randomly deposited EFG sheets as evidenced from SEM analysis of the film edges (Figure 2b) and a very weak (002) reflection characteristic of the graphite layers in the X-ray diffraction (XRD) pattern (Figure 2c). Concentrated EFG solutions of 0.1 mg/mL can be readily prepared by dispersing the EFG film in DMF with no significant sedimentation observed after standing for three weeks (Figure 2d).

XPS analysis of the functionalized graphene films demonstrated a controllable degree of functionalization as a function of the bromine signal at varying electrochemical functionalization times. In contrast, the bromine content does not increase with longer functionalization times for CFGs (Figure 3a).

dx.doi.org/10.1021/ja309023f | J. Am. Chem. Soc. 2012, 134, 17896−17899

Table 1. Weight of Graphite Foil (GF) Electrodes/Immersed GF Electrodes and Functionalized Graphene (G) Film Products, Their Supernatant Concentrations, Reaction Yields, and Summary of Their Chemical and Physical Properties

samples	Wt. of GF/immersed GF (mg)	Wt. of G film (mg)	concentration (μg/mL)	TGA wt % at 500 °C	yield (%)	XPS Br atom %	film resistance (Ω/sq)
EFG (4h)	14.6/8.6	3.8	22	70	31	5.2	8300
EFG (1h)	15.8/9.3	4.6	27	80	40	2.8	8200
CFG (4h)	17.7/10.4	4.4	26	80	34	2	270

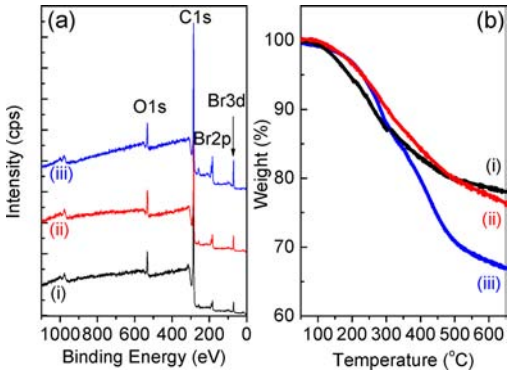

Figure 3. (a) XPS survey scans and (b) TGA spectrum of (i) chemically functionalized graphene with reaction time of 4 h and electrochemically functionalized graphene with reaction time of (ii) 1 h and (iii) 4 h.

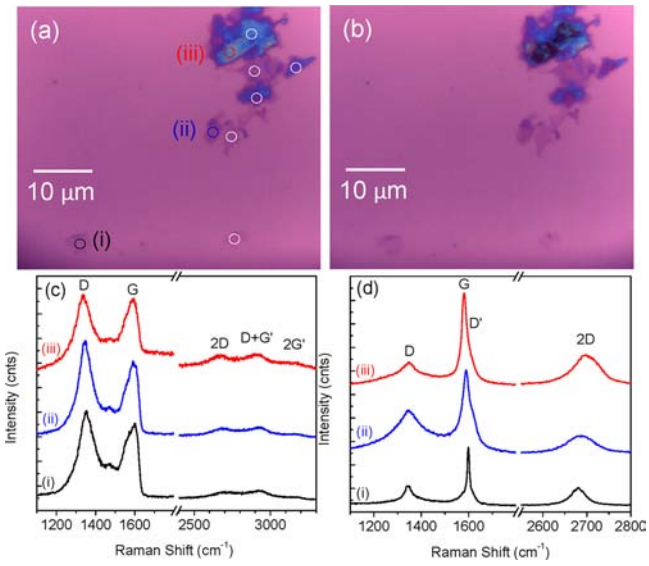

Figure 4. Optical micrograph of EFG spin-coated on silicon (a) before and (b) after laser ablation. Raman spectra of selected spots (i) to (iii) as marked in panel a (c) before and (d) after laser ablation.

Thermal gravimetric analysis (TGA) weight loss measured at 500 °C provides a representative measure of the weight percentage of functional groups in each of the functionalized samples (Figure 3b). The most distinct difference between the EFG and CFG films was that the CFG film displayed a sheet resistance an order in magnitude lower than that of the EFG film (Table 1). This implies a lower degree of basal plane functionalization on the CFG and a higher degree of direct contact between restacked graphene sheets (both contribute to the sheet resistance), which is consistent with the stronger XRD (002) reflection (Figure 2c) as compared to the EFG films. On the basis of product weight of the functionalized graphene films and their respective graphene contents from TGA, the calculated yields of functionalized graphene were in the range of 30 to 40% (Table 1). These values are a lower estimate as only a single extraction of the total solids with DMF has been performed and sonication was kept to a minimum to avoid defects. There are many factors such as the counter electrode, electrolyte concentration, electrolysis voltage, and reaction time that could be further optimized in future studies to provide improved yields. Nevertheless, the present procedure based on two-electrode system is compatible with industrial electrolyzers for ease of scale up.

EFG dispersions (0.1 mg/mL in DMF) were spin-coated on silicon wafers (300 nm oxide layer) for characterization with optical microscopy and Raman spectroscopy. Optical micrographs of the spin-coated EFG (Figure S2) show coverage of the substrate with micrometer-sized graphene flakes with predominantly light blue color over a large area (10× magnification) and also flakes that appear as light gray areas at higher magnifications. Raman spectra of these EFG flakes (Figure 4c and Figure S3) shown in Figure 4a were obtained with a laser spot size of 2 μm. The I_D/I_G ratios of all the EFG flakes were consistently found to be higher than 1.1 indicating that a high degree of covalent functionalization was achieved for all observed graphene flakes. High power laser ablation (>100 mW) was subsequently performed on previously analyzed spots and distinguishable laser "burn marks" were noted on the light blue color EFG flakes (Figure 4b). The postlaser ablation Raman analysis of all the spots revealed significantly reduced D peaks confirming the removal of covalently attached organic functional groups and restoration to near pristine graphene sheets (Figure 4d and Figure S3). By contrast, the D peak of graphene oxide (GO) was reported to remain high after laser ablation, as a result of the presence of irreparable structural edge defects and the smaller graphene domains.[19] The narrowing of the G band after laser treatment to a single sharp peak is also indicative of a carbon state transition from an amorphous to a crystalline state.[20] We also noted the emergence of a sharp symmetrical 2D peak at 2680 cm^{-1} in some of the analyzed flakes, which is indicative of single layer graphene. On the basis of the 2D spectral shape observed in the rest of the graphene flakes, we conclude that all the graphene flakes in the EFG film product are less than five layers.[21]

In conclusion, we have shown the enhancement of electrochemical expansion of graphite via a two step process. This hyperexpanded EEG undergoes enhanced subsequent electrochemical functionalization with diazonium salts. The improved functionalization is attributed to the presence of the electrochemically generated SEI layers within the graphite lattices which acted as stable spacers. The versatility to perform subsequent electrochemical functionalizations on the hyperexpanded and electrically connected EEG is not limited to diazonium chemistry, and provides a scalable route to the production of new graphene and nanocomposite materials.

dx.doi.org/10.1021/ja309023f | J. Am. Chem. Soc. 2012, 134, 17896−17899

■ ASSOCIATED CONTENT

Supporting Information

Experimental, instrumentation details and supporting figures. This material is available free of charge via the Internet at http://pubs.acs.org.

■ AUTHOR INFORMATION

Corresponding Author

tswager@mit.edu

Notes

The authors declare no competing financial interest.

■ ACKNOWLEDGMENTS

This research was supported in part by the Institute for Soldier Nanotechnologies under U.S. Army Research Office under contract W911NF-07-D-0004.

■ REFERENCES

(1) Novoselov, K. S.; Geim, A. K.; Morozov, S. V.; Jiang, D.; Zhang, Y.; Dubonos, S. V.; Grigorieva, I. V.; Firsov, A. A. *Science* **2004**, *306*, 666.

(2) Geim, A. K.; Novoselov, K. S. *Nat. Mater.* **2007**, *6*, 183.

(3) Geim, A. K. *Science* **2009**, *324*, 1530.

(4) Bae, S.; Kim, H.; Lee, Y.; Xu, X.; Park, J.-S.; Zheng, Y.; Balakrishnan, J.; Lei, T.; Kim, H. R.; Song, Y. I.; Kim, Y.-J.; Kim, K. S.; Özyilmaz, B.; Ahn, J.-H.; Hong, B. H.; Iijima, S. *Nat. Nanotechnol.* **2010**, *5*, 574.

(5) Emtsev, K. V.; Bostwick, A.; Horn, K.; Jobst, J.; Kellogg, G. L.; Ley, L.; McChesney, J. L.; Ohta, T.; Reshanov, S. A.; Röhrl, J.; Rotenberg, E.; Schmid, A. K.; Waldmann, D.; Weber, H. B.; Seyller, T. *Nat. Mater.* **2009**, *8*, 203.

(6) Stankovich, S.; Dikin, D. A.; Piner, R. D.; Kohlhaas, K. A.; Kleinhammes, A.; Jia, Y.; Wu, Y.; Nguyen, S. T.; Ruoff, R. S. *Carbon* **2007**, *45*, 1558.

(7) Dikin, D. A.; Stankovich, S.; Zimney, E. J.; Piner, R. D.; Dommett, G. H. B.; Evmenenko, G.; Nguyen, S. T.; Ruoff, R. S. *Nature* **2007**, *448*, 457.

(8) Gómez-Navarro, C.; Weitz, R. T.; Bittner, A. M.; Scolari, M.; Mews, A.; Burghard, M.; Kern, K. *Nano Lett.* **2007**, *7*, 3499.

(9) Hernandez, Y.; Nicolosi, V.; Lotya, M.; Blighe, F. M.; Sun, Z.; De, S.; McGovern, I. T.; Holland, B.; Byrne, M.; Gun'Ko, Y. K.; Boland, J. J.; Niraj, P.; Duesberg, G.; Krishnamurthy, S.; Goodhue, R.; Hutchison, J.; Scardaci, V.; Ferrari, A. C.; Coleman, J. N. *Nat. Nanotechnol.* **2008**, *3*, 563.

(10) Lotya, M.; Hernandez, Y.; King, P. J.; Smith, R. J.; Nicolosi, V.; Karlsson, L. S.; Blighe, F. M.; De, S.; Wang, Z.; McGovern, I. T.; Duesberg, G. S.; Coleman, J. N. *J. Am. Chem. Soc.* **2009**, *131*, 3611.

(11) Li, X.; Zhang, G.; Bai, X.; Sun, X.; Wang, X.; Wang, E.; Dai, H. *Nat. Nanotechnol.* **2008**, *3*, 538.

(12) Englert, J. M.; Dotzer, C.; Yang, G.; Schmid, M.; Papp, C.; Gottfried, J. M.; Steinrück, H.-P.; Spiecker, E.; Hauke, F.; Hirsch, A. *Nat. Chem.* **2011**, *3*, 279.

(13) Shih, C.-J.; Vijayaraghavan, A.; Krishnan, R.; Sharma, R.; Han, J.-H.; Ham, M.-H.; Jin, Z.; Lin, S.; Paulus, G. L. C.; Reuel, N. F.; Wang, Q. H.; Blankschtein, D.; Strano, M. S. *Nat. Nanotechnol.* **2011**, *6*, 439.

(14) Su, C.-Y.; Lu, A.-Y.; Xu, Y.; Chen, F.-R.; Khlobystov, A. N.; Li, L.-J. *ACS Nano* **2011**, *5*, 2332.

(15) Wang, J.; Manga, K. K.; Bao, Q.; Loh, K. P. *J. Am. Chem. Soc.* **2011**, *133*, 8888.

(16) Xu, K. *Chem. Rev.* **2004**, *104*, 4303.

(17) Sirisaksoontorn, W.; Adenuga, A. A.; Remcho, V. T.; Lerner, M. M. *J. Am. Chem. Soc.* **2011**, *133*, 12436.

(18) Eggert, G.; Heitbaum, J. *Electrochim. Acta* **1986**, *31*, 1443.

(19) Strong, V.; Dubin, S.; El-Kady, M. F.; Lech, A.; Wang, Y.; Weiller, B. H.; Kaner, R. B. *ACS Nano* **2012**, *6*, 1395.

(20) Kudin, K. N.; Ozbas, B.; Schniepp, H. C.; Prud'homme, R. K.; Aksay, I. A.; Car, R. *Nano Lett.* **2007**, *8*, 36.

(21) Malarda, L. M.; Pimenta, M. A.; Dresselhaus, G.; Dresselhaus, M. S. *Phys. Rep.* **2009**, *473*, 51.